HHS Public Access

Author manuscript

Cell Host Microbe. Author manuscript; available in PMC 2019 February 14.

Published in final edited form as:

Cell Host Microbe. 2018 February 14; 23(2): 177–190.e4. doi:10.1016/j.chom.2018.01.001.

Loss of Paneth cell autophagy causes acute susceptibility to *Toxoplasma gondii*-mediated inflammation

Elise Burger[1], **Alessandra Araujo**[1], **Américo López-Yglesias**[1], **Michael W. Rajala**[2], **Linda Geng**[3], **Beth Levine**[3,4,5], **Lora V. Hooper**[5,6], **Ezra Burstein**[3], and **Felix Yarovinsky**[1,7,*]

[1]Center for Vaccine Biology and Immunology, Department of Microbiology and Immunology, University of Rochester Medical Center, Rochester, NY, 14642, USA

[2]Department of Internal Medicine, University of Michigan, Ann Arbor, MI, 48109, USA

[3]Department of Internal Medicine, The University of Texas Southwestern Medical Center, Dallas, TX, 75390, USA

[4]Center for Autophagy Research, The University of Texas Southwestern Medical Center, Dallas, TX, 75390, USA

[5]Howard Hughes Medical Institute, The University of Texas Southwestern Medical Center, Dallas, TX, 75390, USA

[6]Department of Immunology, The University of Texas Southwestern Medical Center, Dallas, TX 75390, USA

[7]Lead Contact

Summary

The protozoan parasite *Toxoplasma gondii* triggers severe small intestinal immunopathology characterized by IFN-γ- and intestinal microbiota-mediated inflammation, Paneth cell loss and bacterial dysbiosis. Paneth cells are a prominent secretory epithelial cell type that reside at the base of intestinal crypts and release antimicrobial peptides. We demonstrate that the microbiota triggers basal Paneth cell-specific autophagy via induction of IFN-γ, a known trigger of autophagy, to maintain intestinal homeostasis. Deletion of the autophagy protein Atg5 specifically in Paneth cells results in exaggerated intestinal inflammation characterized by complete destruction of the intestinal crypts resembling that seen in pan-epithelial Atg5-deficient mice. Additionally, lack of functional autophagy in Paneth cells within intestinal organoids and *T. gondii*-infected mice causes increased sensitivity to the proinflammatory cytokine TNF along with

*Correspondence: felix_yarovinsky@URMC.Rochester.edu.

Author Contributions

E.B., A.A., F.Y., designed experiments; E.B., A.A., A.L.Y, and L.G. performed experiments; M.W.R., B.L., L.V.H., and E.B. provided critical reagents and scientific insight; E.B., A.A., A.L.Y., and F.Y. analyzed data; E.B. and F.Y. wrote the paper.

Declaration of Interests

The authors declare no competing interests

increased intestinal permeability, leading to exaggerated microbiota- and IFN-γ-dependent intestinal immunopathology. Thus, Atg5 expression in Paneth cells is essential for tissue protection against cytokine-mediated immunopathology during acute gastrointestinal infection.

Abstract

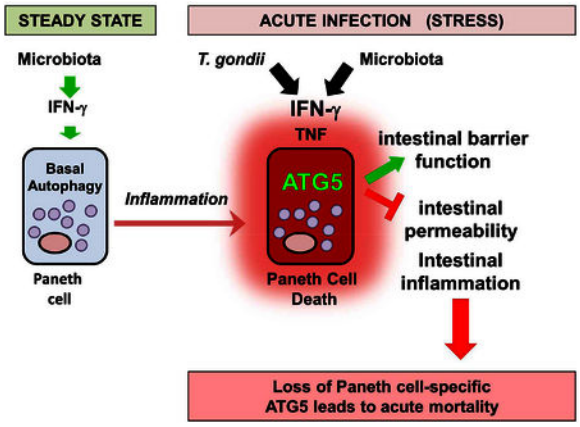

Introduction

Intestinal homeostasis relies on the cooperation of multiple cell types in the intestinal epithelium with local immune cells and the gut microbiota. The intestinal epithelium, comprised of absorptive enterocytes along with Paneth, goblet, tuft, and enteroendocrine cells, acts as a physical barrier between the host and the resident gut bacterial populations (Peterson and Artis, 2014). Of these epithelial cells, Paneth cells are the dominant secretory cells found at the base of the intestinal crypts in the small intestine. These cells secrete antimicrobial peptides, including lysozyme and cryptdins into the lumen (Clevers and Bevins, 2013), which are critical for regulating the microbiota composition (Salzman et al., 2010; Salzman et al., 2007).

In addition to antimicrobial peptides (AMPs), several cytokines, in particular IL-17, IL-22, and IFN-γ, play an indispensable role in intestinal homeostasis and inflammation (Dudakov et al., 2015; Ivanov et al., 2006; Strober et al., 2007; Weaver et al., 2013). Both *in vitro* (Farin et al., 2014) and *in vivo* (Raetz et al., 2013) experiments revealed that high levels of IFN-γ triggered by microbial infection can lead to Paneth cell loss. *In vivo* experiments with the protozoan parasite *T. gondii* revealed that the loss of Paneth cells is an element of the highly polarized Th1 response to the parasite along with severe intestinal inflammation and dysbiosis (Belkaid and Hand, 2014; Raetz et al., 2013). However, the precise connection between the microbiota, proinflammatory cytokines and Paneth cell loss is still not completely understood (McSorley and Bevins, 2013).

Among multiple cellular responses, IFN-γ is known as a potent inducer of autophagy, an evolutionarily ancient catabolic process that helps maintain cellular function during stress by recycling intracellular components (Gutierrez et al., 2004; Harris, 2011; Matsuzawa et al., 2012). In this process, part of the cytoplasm is surrounded by a double-membrane

autophagosome. Fusion with a lysosome generates an autolysosome, which enzymatically degrades the contents within (Levine et al., 2011). This mechanism requires coordination of many proteins for proper targeting and degradation. Atg5 and Atg12 interact with the elongating isolation membrane and LC3 becomes lipid-conjugated and associated with the mature autophagosome membrane (Mizushima, 2002). In addition to balancing cell death and proliferation (Deretic and Levine, 2009; Levine et al., 2011; Patel and Stappenbeck, 2013), autophagy is indispensable for resistance to intestinal pathogens including *T. gondii* (Choi et al., 2014; Ling et al., 2006; Selleck et al., 2015; Zhao et al., 2008), *L. monocytogenes* (Gupta et al., 2015; Py et al., 2007; Zhao et al., 2008), and *S. typhimurium* (Benjamin et al., 2013; Conway et al., 2013; Hernandez et al., 2003; Jia et al., 2009). Dysregulation of autophagy in the intestinal epithelial compartment is also implicated in inflammatory bowel disease (IBD) (Lassen et al., 2016; Patel and Stappenbeck, 2013; Rioux et al., 2007). Studies examining polymorphisms in multiple genes linked to Crohn's disease susceptibility, including *NOD2, ATG16L1* and *IRGM*, have revealed a key role for autophagy in regulating Paneth cell function (Cadwell et al., 2008; Cadwell et al., 2009c; Liu et al., 2013; Zhang et al., 2015).

Mice deficient in Atg16l1 in the intestinal epithelium display significant defects localized to the Paneth cell granule exocytosis pathway, resulting in decreased AMP secretion (Cadwell et al., 2008). Additionally, Atg16l1 along with the upstream autophagy protein Atg7 play a compensatory role against endoplasmic reticulum stress and help maintain homeostasis in the intestinal epithelium (Adolph et al., 2013). Examination of the autophagy pathway in mice lacking Atg7 and Atg5 in the intestinal epithelium revealed Paneth cell abnormalities indistinguishable from the Atg16l1 mice (Cadwell et al., 2009a). While Atg5 is uniquely capable of additional autophagy-independent functions in phagocytic cells (Kimmey et al., 2015; Zhao et al., 2008), the analogous impact on Paneth cells from deficiency in Atg5, Atg7, or Atg16 suggests that the primary function of Atg5 in Paneth cells is to control the autophagy pathway.

Despite a well-appreciated role for autophagy in Paneth cell function under steady state conditions (Stappenbeck, 2010), the potential immunoregulatory role of autophagy in Paneth cells during inflammatory insults has not been sufficiently explored. Here we show that Paneth cell-intrinsic autophagy is driven by the intestinal microbiota via induction of the basal levels of IFN-γ. Intact Paneth cell-intrinsic autophagy is indispensable for tissue homeostasis in response to inflammatory insult caused by *T. gondii* infection. Atg5 deficiency only in Paneth cells resulted in acute mortality of the infected mice caused by uncontrolled IFN-γ and TNF mediated immunopathology triggered by the parasite.

Results

Steady state Paneth cell specific autophagy depends on the microbiota and IFN-γ

Autophagy is a highly specialized cellular process required for the recycling of intracellular components (Mizushima, 2007). The functional autophagic machinery requires cooperation between multiple proteins which generate the double membrane-bound structures in the cytosol that are ultimately delivered to lysosomes for recycling (Deretic et al., 2013; Mizushima, 2007). Among these, the membrane protein LC3 fused to GFP allows for

identification of cells undergoing autophagy *in vivo* (Mizushima, 2009; Mizushima et al., 2004).

While autophagy plays an indispensable role for host defense and homeostatic functions of all enterocytes, intact autophagy is essential for Paneth cell functionality (Adolph et al., 2013; Cadwell et al., 2008; Cadwell et al., 2009a; Deuring et al., 2014; Kaser and Blumberg, 2014; Lassen et al., 2014; Liu et al., 2013; Ouellette, 2010; Salas and Panes, 2009; Stappenbeck and McGovern, 2016), even though the mechanisms that regulate autophagy in these cells are understood incompletely.

Analysis of small intestinal crypts in naïve GFP-LC3 mice revealed that Paneth cells, identified by *Ulex europaeus* agglutinin 1 lectin (UEA-1), undergo autophagy during steady state conditions, detected by the presence of GFP-LC3 puncta (Fig. 1A). GFP-LC3 puncta were not detected in the remaining intestinal epithelial cells, suggesting that under steady state conditions, autophagy is more active in Paneth cells than other intestinal epithelial cell populations (Fig. 1A, B).

The epithelial layer of the small intestine is constantly exposed to the microbial products derived from the intestinal microbiota (Peterson and Artis, 2014). Innate sensing of the microbiota leads to complex epithelial cell-intrinsic and -extrinsic responses characterized by production of antimicrobial peptides and cell proliferation as is evident from the analysis of microbiologically sterile germ-free mice, conventional mice treated with antibiotics, or animals with deleted innate immune sensors and their adaptor proteins (Belkaid and Hand, 2014; Benson et al., 2009; Kaiko and Stappenbeck, 2014; Kelsall, 2008; Kirkland et al., 2012; Peterson and Artis, 2014). We observed that depletion of the microbiota by antibiotic treatment resulted in a dramatic decrease in GFP-LC3 puncta in Paneth cells compared to untreated controls (Fig. 1C-D). This was characterized both as a decrease in the number of GFP-LC3-positive Paneth cells per intestinal crypt and a striking reduction in the number of GFP-LC3 puncta within each Paneth cell (Fig. 1D-E). These results suggest that basal autophagy in Paneth cells depends on the presence of the microbiota.

The microbiota has a pleiotropic effect on mucosal immunity, including induction of cytokines that regulate Paneth cells functions (Bevins and Salzman, 2011). We observed that antibiotic-mediated depletion of the microbiota results in dramatically reduced levels of the basal IFN-γ (Fig. 1F), a key cytokine for inducing autophagy (Feng et al., 2009; Gutierrez et al., 2004; Ling et al., 2006; Matsuzawa et al., 2012; Selleck et al., 2015). Similar observations were made in microbiologically sterile germ-free mice that lack intestinal bacteria (Fig. 1G). In these mice the lack of intestinal bacteria compromised the basal host IFN-γ response. These results prompted us to examine if basal levels of IFN-γ triggered by the microbiota play a role in the induction of Paneth cell autophagy. The presence of GFP-LC3 puncta were next analyzed in the small intestine of GFP-LC3 mice treated with IFN-γ blocking antibody. We observed a marked reduction of GFP-LC3 puncta in Paneth cells in mice treated with IFN-γ blocking but not control antibody (Fig. 1H,I,J). These experiments indicate that the microbiota-driven basal autophagy observed in Paneth cells depends on IFN-γ.

Loss of intestinal epithelial Atg5 leads to a catastrophic susceptibility to *T. gondii*-infection

The experiments from our and other laboratories have demonstrated that epithelial cell exposure to high levels of IFN-γ results in rapid Paneth cell loss and severe intestinal inflammation (Farin et al., 2014; Raetz et al., 2013). Combined with the observation of IFN-γ-dependent autophagy induction in Paneth cells (Fig. 1), we hypothesized that the Paneth cell-specific autophagic response triggered by excessive amounts of IFN-γ is a mechanism that contributes to intestinal inflammation during *T. gondii* infection. To test this possibility, mice with an intestinal epithelial cell-restricted deficiency in autophagy achieved by the deletion of Atg5 using the Villin-Cre deleter (Villin-Cre x $Atg5^{flox/flox}$ mice, E-Atg5 KO) were orally infected with *T. gondii*. We anticipated that lack of Atg5 would limit IFN-γ-mediated intestinal inflammation by preventing autophagy-mediated loss of Paneth cells. Contrary to our prediction, epithelial cell-restricted Atg5 deficiency resulted in acute susceptibility not seen in the control mice (Fig. 2A). The observed early mortality of E-Atg5 KO mice prompted us to further investigate the fate of Paneth cells in these mice. First, we examined naïve E-Atg5 KO mice and in agreement with previous reports, epithelial cell-intrinsic autophagy was not required for the development of Paneth cells but played a role in their ability to produce AMPs (Cadwell et al., 2008; Lassen et al., 2014). This was evident as a similar number of Paneth cells per intestinal crypt were seen in E-Atg5 KO mice when compared to WT controls (Supplemental Fig. 1A,B). Examination of two representative Paneth cell-specific antimicrobial peptides, Defcr2 and Defa6, revealed that naïve E-Atg5 KO mice have partially reduced expression of AMPs compared to WT mice (Supplemental Fig. 1C).

A thorough histologic examination of small intestines isolated from *T. gondii*-infected mice revealed that Atg5-sufficient mice develop substantial inflammatory cell infiltrates, but overall preserved structure and integrity of the epithelium (Fig. 2B). In striking contrast, E-Atg5 KO mice exhibited extreme immunopathology throughout the entire small intestine. All crypts in *T. gondii* infected E Atg5 KO mice were completely destroyed, with only inflammatory infiltrates remaining (Fig. 2B). Thus, loss of Atg5 in the small intestinal epithelium leads to a substantial increase in susceptibility to *T. gondii*-mediated intestinal damage.

In addition to the severe intestinal inflammation, *T. gondii* infection resulted in a complete loss of Paneth cells in the intestines of E-Atg5 KO mice (Fig. 2C). This was particularly evident by histological analysis of the glycoproteins in the cells of small intestine that allows the definitive histological identification of Paneth cells (Fig. 2D-F).

Loss of intestinal epithelial Atg5 does not lead to uncontrolled *T. gondii* pathogen burden or to elevated IFN-γ production.

Intact expression of Atg5 is known to be essential for *in vivo* resistance to the intracellular pathogens including *T. gondii*, since the lack of Atg5 in macrophages prevents IFN-γ-induced parasite clearance (Zhao et al., 2008). We next examined if similar to myeloid cells, epithelial cell-intrinsic Atg5 is involved in controlling *T. gondii* parasites. Our experiments revealed that deletion of Atg5 in epithelial cells has no effect on *T. gondii* pathogen burden measured in all examined tissues, including liver and spleen (Fig. 2G, H).

To determine if the enhanced mortality and intestinal pathology in E-Atg5 KO mice is caused by uncontrolled production of IFN-γ, we next compared the levels of IFN-γ triggered by *T. gondii* infection in WT and E-Atg5 KO mice. We observed that both the expression levels in the intestine and the amount of secreted IFN-γ detectable in blood were indistinguishable between the experimental groups (Fig. 2I, J). Furthermore, no difference in induction of Th1 cells was detected in draining lymph nodes and spleens of *T. gondii*-infected E-Atg5 KO and WT mice (Supplemental Fig. 2A-C). These results ruled out a possibility that uncontrolled expression of IFN-γ might result in enhanced intestinal immunopathology and loss of Paneth cells in E-Atg5 KO mice infected with *T. gondii*. We also observed no difference in the absolute numbers of the examined infiltrating cells in the lamina propria of small intestines among *T. gondii*-infected WT and E-Atg5 KO mice (Supplemental Fig. 3).

In the search for the factors that could explain the enhanced susceptibility of the autophagy-deficient mice to *T. gondii*, we observed that TNF expression levels in intestines of naïve E-Atg5 KO mice were significantly elevated in comparison to naïve WT counterparts (Fig. 2K). During oral *T. gondii* infection, infected E-Atg5 KO mice demonstrated a further increase in TNF levels compared to WT mice infected with the parasite (Fig. 2K). Combined with the previous reports describing a major role for TNF in intestinal inflammation (Egan et al., 2009; Liesenfeld, 2002; Liesenfeld et al., 1999), our data prompted us to investigate if enhanced intestinal pathology and loss of Paneth cells in E-Atg5 KO mice is in part due to exaggerated TNF elevation caused by the parasitic infection.

Autophagy-deficient intestinal organoids exhibit enhanced susceptibility to cytokine-mediated cell death

To assess if Atg5 deficiency influences the sensitivity of Paneth cells to TNF, we took advantage of intestinal organoids as an experimental system to examine the sensitivity of Paneth cells to TNF-dependent intestinal inflammation in the presence or absence of functional cell-intrinsic Atg5. In this system Paneth cells were visualized by light microscopy as granule-containing cells in the budding crypt-like structures of the organoids developed from both WT and Atg5-deficient epithelial stem cells (black arrowheads, Fig. 3A). The presence of Paneth cells in organoids generated from both WT and E-Atg5 KO mice was verified by immunofluorescence utilizing UEA-1 in combination with lysozyme staining, which is a Paneth cell-specific AMP (yellow arrowheads, Fig. 3A). To induce intestinal cell death, the intestinal organoids generated from WT or E-Atg5 KO mice were treated with TNF (Fig. 3B). We observed that while twelve hour TNF stimulation alone resulted in minimal WT organoid death, similar treatment resulted in death of half of E-Atg5 KO organoids (Fig. 3B, C). Extending TNF stimulation time to 24 hours led to nearly complete death in the E-Atg5 KO organoids, whereas the WT organoids remained alive and intact (Supplemental Fig. 4). Organoid death was quantified as loss of epithelial integrity and impaired lumen formation associated with the appearance of the individual cells and debris seen on the exterior of the organoid.

To recapitulate intestinal inflammation in the presence of IFN-γ, intestinal organoids were exposed to IFN-γ. We observed that IFN-γ stimulation failed to cause the death of the

intestinal organoids (Fig 3B,C), but instead resulted in the progressive and selective loss of Paneth cells, but no difference in the cytokine-induced cell death was observed between WT and Atg5-deficient organoids (Fig. 3D and data not shown). Combination of TNF with IFN-γ led to an increase in organoid death versus TNF alone in both strains of organoids, revealing that IFN-γ potentiated the sensitivity to cell death (Fig. 3B,C). Overall, these results revealed that epithelial cell-restricted Atg5 deficiency resulted in increased sensitivity to TNF-mediated cell death.

Immunopathology of Atg5 deficiency originates from Paneth cells

A major inadequacy of the use of E-Atg5 KO mice is that while pan-epithelial deletion of Atg5 targets Paneth cells, it is not restricted to this cell type. This substantially limits interpretations that the observed enhanced immunopathology and susceptibility to *T. gondii* of E-Atg5 KO mice are the result of impaired autophagic machinery in Paneth cells. To overcome this limitation, we generated Paneth-cell specific Atg5-deficient mice by crossing the same $Atg5^{Flox/Flox}$ mice with αDefensin4-IRES-Cre knock-in animals (PC-Atg5 KO mice, Supplemental Fig. 5). Due to the Paneth cell-restricted expression of αDefensin-4, Cre recombinase is selectively expressed in Paneth cells in these mice as is evident from the analysis of αDefensin4 -IRES-Cre x TdTomato-Rosa26 reporter (Fig. 4A). In these reporter mice TdTomato expression was limited to lysozyme-expressing Paneth cells located at the base of the intestinal crypts and was not detected in any other examined cell type (Fig. 4 and data not shown). Furthermore, similar to Atg16L1-deficient mice (Cadwell et al., 2008), the Paneth cell-specific deletion of Atg5 resulted in notable abnormalities in granule morphology, specifically hypomorphic and reduced granule numbers per Paneth cell without affecting the total numbers of Paneth cells in naïve PC-Atg5 KO mice (Fig. 4B,C). Similarly to E-Atg5 KO mice, PC-Atg5 KO mice exhibit partially reduced expression of AMPs such as Defcr2 (Fig. 4D).

The Paneth cell-specific reporter mice infected with *T. gondii* provided direct evidence for the Paneth cell loss in response to *T. gondii* infection, since in addition to the loss of the RNA transcripts for the Paneth cell-specific AMPs, we observed both nearly complete disappearance of TdTomato+ cells by immunofluorescence and the RNA transcript for the Cre recombinase selectively expressed in Paneth cells in response to *T. gondii* infection (Fig. 4E-G). Most importantly, when PC-Atg5 KO mice were infected with *T. gondii*, the observed intestinal pathology largely recapitulated the phenotype seen in E-Atg5 KO mice. Similar to E-Atg5 KO mice, all crypts and Paneth cells in *T. gondii*-infected PC-Atg5 KO mice were completely destroyed (Fig. 5A). We also observed that PC-Atg5 KO mice are highly susceptible to *T. gondii* and their mortality was only slightly delayed when compared to E-Atg5 KO mice (Fig. 5B). These results established both a crucial role for Atg5 in Paneth cells, and also suggest that Atg5 plays additional functions in other epithelial cells important for host defense (Fig 5B). Similar to E-Atg5 KO mice, the Paneth cell-specific abrogation of Atg5 was sufficient for the most profound loss of Paneth cells (Fig 5C), but it was not associated with increased parasite burden, systemic dissemination of the intestinal bacteria, or production of IFN-γ and TNF by CD4+ T cells at the site of infection (Fig. 5D-G). Instead, we observed that Paneth cell-specific disruption of Atg5 was sufficient for the impaired control of the luminal bacteria that were in close contact with the intestinal

epithelial cells in *T. gondii*-infected E-Atg5 KO and PC-Atg5 KO mice (Fig. 5H). The lack of Atg5 in Paneth cells or all intestinal enterocytes shortened the distance separating villi from the microbiota (Fig 5H, I). Furthermore, lack of Atg5 in Paneth cells resulted in impaired intestinal barrier function as was evident from the increased intestinal permeability measured by a FITC-labeled dextran method (Fig 5J), and the appearance of LPS in the circulation of E-Atg5 KO and PC-Atg5 KO mice infected with *T. gondii* (Fig. 5K). Thus, the use of PC-Atg5 KO mice revealed that the lack of Atg5 only in Paneth cells exacerbated the intestinal immunopathology caused by *T. gondii* infection and was sufficient for the acute mortality of mice during the parasitic infection.

Intestinal inflammation in Atg5-deficient intestines is driven by the microbiota

Our previous experiments revealed that microbiologically sterile germ-free mice infected with *T. gondii* retain their Paneth cells and do not develop intestinal inflammation (Raetz et al., 2013). Combined with our observation that *T. gondii* infection results in impaired intestinal control of microbiota (Fig. 5H, I) and increased intestinal permeabilization (Fig. 5J, K), we examined if depletion of the intestinal microbiota by antibiotics prevents the loss of Paneth cells in *T. gondii*- infected E-Atg5 KO and PC-Atg5 KO mice.

We observed that reduction of intestinal microbiota resulted in greatly weakened Th1 responses in all experimental groups independently of Atg5 expression in Paneth cells or all epithelial cells (Fig. 6A-D and Supplemental Fig. 6). Similar to WT controls, both E-Atg5 KO and PC-Atg5 KO mice developed an attenuated Th1 response when intestinal bacteria were depleted by antibiotic treatment. Furthermore, lack of intestinal bacteria completely prevented the loss of Paneth cells even in the absence of Atg5 (Fig. 6E). This was evident from the quantification of Paneth cells in the intestinal crypts and during the analysis of the RNA transcripts for the Paneth cell specific proteins (Fig. 6F, G) that correlated with the abolished intestinal IFN-γ production in the antibiotic-treated mice (Fig. 6H), further emphasizing a crucial role for this cytokine in the regulation of Paneth cell biological functions.

Inflammatory cytokines are critical mediators of *T. gondii*-mediated pathology

Next we formally examined the contributions of TNF and IFN-γ in driving intestinal pathology in E-Atg5 KO and PC-Atg5 KO mice. Control, E-Atg5 KO, and PC-Atg5 KO mice were infected with *T. gondii* alone or with the additional supplementation of TNF or IFN-γ blocking antibodies. As expected, all WT controls developed intestinal inflammation that was completely prevented with anti-IFN-γ antibody (Fig. 7A-C). In addition, anti-TNF treatment attenuated inflammation and partially prevented the loss of Paneth cells in WT mice. Similarly to the control mice, anti-IFN-γ treatment during *T. gondii* infection resulted in the prevention of the Paneth cell loss in both E-Atg5 KO and PC-Atg5 KO. In addition, similar to the results with the intestinal organoids, TNF was responsible for the loss of the intestinal architecture in both E-Atg5 KO and PC-Atg5 KO mice, as anti-TNF treatment decreased the intestinal pathology, even though it was not sufficient to prevent the loss of Paneth cells caused by *T. gondii* infection (Fig. 7).

Overall, our experiments established that intestinal microbiota drives the autophagy in Paneth cells via induction of basal levels of IFN-γ. At the same time, Paneth cell autophagy is essential for the regulation of epithelial homeostasis during type I intestinal inflammation caused by IFN-γ in part by to the regulation of the local epithelial cell-mediated control of the intestinal bacteria and regulation of Paneth cell responsiveness to TNF. The lack of Atg5 specifically in Paneth cells results in the microbiota-dependent IFN-γ and TNF-mediated intestinal damage during infection with a common parasite *T. gondii* that leads to lethal intestinal permeability. Taken together, we revealed a protective role for Paneth cell-intrinsic expression of Atg5 in preserving tissue integrity in response to cytokine-mediated inflammation.

Discussion

The use of autophagy reporter and Paneth cell-intrinsic Atg5 deficient mice allowed us to identify that under steady state conditions, intestinal microbiota-driven IFN-γ is a central inducer of Paneth cell autophagy. The protective role of autophagy in epithelial homeostasis was revealed during acute mucosal responses to a protozoan parasite *T. gondii in vivo* and in intestinal organoids *in vitro*. Epithelial cell- and Paneth cell-restricted Atg5 deficiency results in susceptibility to *T. gondii* associated with severe immunopathological changes in the small intestine of infected mice. Intestinal organoids further proved an essential role of autophagy in resistance to cytokine-mediated epithelial cell death.

Autophagy is a fundamental cellular process required for the recycling of intracellular components. It is indispensable for a variety of developmental processes, regulating cellular stress and orchestrating host defense responses (Deretic et al., 2013). Immunity to all groups of pathogens, including prions (Heiseke et al., 2010), viruses (Dong and Levine, 2013), bacteria (Benjamin et al., 2013; Jia et al., 2009; Py et al., 2007), and parasites (Choi et al., 2014; Ling et al., 2006; Selleck et al., 2015; Zhao et al., 2008) depends on autophagy to coordinate an immune response that leads to direct or indirect pathogen elimination in infected cells. This is particularly well illustrated in cells infected with *T. gondii*. Stimulation of macrophages by IFN-γ or CD40 leads to the lysosomal destruction of *T. gondii* parasites inside infected cells (Van Grol et al., 2013). More recently it was shown that IFN-γ-dependent control of *T. gondii* in human macrophages depends on ubiquitination and core autophagy proteins that mediate membrane engulfment and restriction of parasite growth (Clough et al., 2016; Coers and Haldar, 2015; Lee et al., 2015; Selleck et al., 2015).

What is less understood are the drivers of autophagy under steady-state and inflammatory conditions, and the broader immunoregulatory role for autophagy in addition to direct pathogen elimination in infected cells. This is especially relevant to Paneth cells, highly specialized cells constitutively producing antimicrobial peptides in small intestine. The importance of the intact autophagy system in Paneth cells is strongly supported by clinical observations, in which polymorphisms in autophagy-associated genes, such as *ATG16L1* and *IRGM*, are linked to Crohn's disease (Cadwell et al., 2009c; Lassen et al., 2014; Liu et al., 2013). Detailed analysis of *Atg16l1* hypomorphic mice revealed an autophagy-dependent mechanism for the accumulation, sorting, and secretion of granules containing the antimicrobial proteins (Cadwell et al., 2008).

In this report we found that basal microbiota-driven production of IFN-γ in the small intestine is a major inducer of autophagy in Paneth cells. Importantly, while treatment of GFP-LC3 mice with IFN-γ blocking antibody did not impact overall Paneth cell numbers, there was a major decrease in GFP-LC3+ Paneth cells. In addition, the remaining GFP-LC3+ Paneth cells showed a dramatic drop in the absolute numbers of autophagic vesicles. These experiments revealed that Paneth cell autophagy, which was previously considered constitutive, is in reality an IFN-γ-inducible mechanism.

This may have a major implication in intestinal homeostasis, since both upregulation of IFN-γ and Paneth cell-specific autophagy are associated with inflammatory bowel disease development (Cadwell et al., 2009c). While the observed intestinal expression of IFN-γ can be induced by multiple factors, antibiotic treatment dramatically reduced the levels of IFN-γ and the appearance of GFP-LC3-containing vesicles, strongly suggesting that the intestinal microbiota is a major factor responsible for the basal autophagy detected in Paneth cells.

We initially hypothesized that additional induction of IFN-γ during the mucosal response to *T. gondii* leads to excessive autophagy activation and unintentional Paneth cell elimination. Contrary to our hypothesis, the experimental analysis of *T. gondii*-infected PC-Atg5 KO and E-Atg5 KO mice revealed that elimination of Atg5 only in Paneth cells or in all enterocytes did not protect Paneth cells from IFN-γ-dependent cell death. Instead, we revealed that the lack of Atg5 resulted in profound intestinal immunopathology characterized by near complete elimination of all epithelial cells, including Paneth cells. It is important to note that the impairment in the intestinal epithelium was not seen in naïve autophagy-deficient mice, suggesting that the noticeable protective effects of epithelial intrinsic Atg5 can in particular be exposed under inducible inflammatory conditions. The elevated levels of TNF seen in naïve PC-Atg5 KO and E-Atg5 KO mice that are further elevated during mucosal response to *T. gondii* are a central element of the immunopathological response seen in the infected mice. This conclusion was confirmed with the *de novo* generated intestinal organoids from E-Atg5 KO and PC-Atg5 KO mice. Most importantly, we revealed a direct connection between microbiota-dependent induction of IFN-γ that plays a key role in the induction of the intestinal tissue-protective autophagy in Paneth cells.

Taken together, our experiments revealed that microbiota- and IFN-γ-driven Paneth cell-specific Atg5 plays a critical immunoregulatory function and protects epithelial cells during acute cytokine-mediated intestinal inflammation.

STAR Methods

CONTACT FOR REAGENT AND RESOURCE SHARING

Further information and requests for resources and reagents should be directed to and will be fulfilled by the Lead Contact, Felix Yarovinsky (felix_yarovinsky@URMC.Rochester.edu)

EXPERIMENTAL MODEL AND SUBJECT DETAILS

Mice—C57BL/6 mice were originally purchased from the Jackson Laboratories and were maintained in the pathogen-free animal facility at the University of Rochester School of Medicine and Dentistry. The breeding pairs of GFP-LC3 mice (Hara et al., 2006) and

Atg5$^{flox/flox}$ x Villin-cre (E-Atg5 KO) mice (Benjamin et al., 2013) were provided by Beth Levine and Lora Hooper (UT Southwestern Medical Center), all on a C57/B6 background. Villin-Cre mice (Madison et al., 2002) were purchased from the Jackson Laboratory. Germ-free C57BL/6 mice were bred and maintained at the University of Rochester School of Medicine and Dentistry. *α Defensin4 IRES-cre* (Paneth cell-specific, PC-cre) mice were backcrossed to B6 mice (N7) and then crossed to *TdTomato-Rosa26* reporter mice (B6 background) to generate *TdTomato-Rosa26/PC-cre* mice and to *Atg5*$^{flox/flox}$ mice to generate *Atg5*$^{flox/flox}$ x Paneth cell-cre (PC-Atg5 KO) mice. Mice for all experiments were age- and sex-matched. This study included both male and female mice, and the data derived from male and female mice identified no sex-specific differences in the performed experiments.

All mice were maintained in the pathogen-free animal facility at the University of Rochester School of Medicine and Dentistry, Rochester, NY. All animal experimentation was conducted in accordance with the guidelines of the University of Rochester's University Committee on Animal Resources (UCAR), the Institutional Animal Care and Use Committee (IACUC). All animal experimentation in this study was reviewed and approved by the University of Rochester's University Committee on Animal Resources (UCAR), the Institutional Animal Care and Use Committee (IACUC).

The genotypes of all mice were verified with the following genotyping primers: GFP-LC3: 5′-ATAACTTGCTGGCCTTTCCACT-3′, 5′-CGGGCCATTTACCGTAAGTTAT-3′ and 5′-GCAGCTCATTGCTGTTCCTCAA-3′; Atg5: 5'-GAATATGAAGGAACACCCCTGAAATG-3', 5′-GTACTGCATAATTGGTTTAACTCTTGC-3' and 5′-ACAACGTCGAGCACAGCTGCGCAAGG-3', Villin-Cre: oIMR0015, 5'-CAAATGTTGCTTGTCTGGTG-3', oIMR0016, 5'-GTCAGTCGAGTGCACAGTTT-3', oIMR1878, 5'-GTGTGGGACAGAGAACAAACC-3', oIMR1879 and 5'-ACATCTTCAGGTTCTGCGGG-3', TdTomato: 5'-AAGGGAGCTGCAGTGGAGTA-3', 5'-CCGAAAATCTGTGGGAAGTC-3', 5'-GGCATTAAAGCAGCGTATCC-3', 5'-CTGTTCCTGTACGGCATGG-3', Generic cre: 5'-GCGGTCTGGCAGTAAAAACTATC-3', 5'-GTGAAACAGCATTGCTGTCACTT-3', 5'-CTAGGCCACAGAATTGAAAGATCT-3', 5'-GTAGGTGGAAATTCTAGCATCATCC-3'.

METHOD DETAILS

***Toxoplasma gondii* infection and histopathology—**Me49 strain *T. gondii* tissue cyst (bradyzoite) stages were maintained through serial passage in Swiss Webster mice. For infections, brains of chronically (three months) infected mice were mechanically separated by passage through a series of 18-gauge, 20-gauge, and 22-gauge needles. Experimental mice were orally infected with 20 *T. gondii* brain cysts (ME49 strain). Portions of small intestine were fixed in Carnoy's fixative, embedded in paraffin and stained with hematoxylin and eosin (H&E) or Alcian blue/Periodic Acid Schiff (PAS). Paneth cells were identified based on their morphology of large granule-containing cells and a basolateral nucleus at the base of the intestinal crypt. Quantification of Paneth cells per intestinal crypt was performed in a double blinded manner.

In some experiments, mice were injected i.p. with 200 μg anti-IFN-γ (clone XMG1.2, BioXCell) or 200 μg αTNF (clone XT3.11, BioXCell) on day 0, 2, 4 and 6 post-infection. Depletion of commensal bacteria was achieved by providing mice with 10 days of antibiotic water containing ampicillin (1 mg/ml), streptomycin (1 mg/ml), neomycin (1 mg/ml), metronidazole (1 mg/ml), and vancomycin (500 μg/ml) as previously described (Kirkland et al., 2012).

For immunofluorescence, small intestines were divided on 16 equal parts and 'segment 8' was used for the analysis after fixation in 4% paraformaldehyde in PBS for 4 hours. Embedded and frozen in OCT compound (Tissue-Tek) intestine sections of 8μm were permeabilized with 0.2% Triton-X in PBS, and blocked with 0.1% Triton-X with 5% Normal Goat Serum in PBS. GFP-LC3 sections were incubated with anti-GFP Alexa Fluor 488 (Molecular Probes) and UEA-TRITC for 1 hour at room temperature, counterstained with Syto62 (Molecular Probes) and mounted in ProLong Gold (Molecular Probes). Specimens were imaged with a Leica SPE system fitted with a Leica 63X objective NA 1.4. Quantification of GFP-LC3+ puncta was performed in a double blinded manner.

TdTomato-Rosa26/PC-cre sections were incubated with primary antibody against lysozyme (rabbit polyclonal; Dako) in 0.05% Triton X-100/PBS overnight at 4°C. Slides were washed and incubated with goat anti-rabbit Alexa Fluor 488 (Molecular Probes) for 1 hour at room temperature. After washing, nuclei were stained with DAPI (Sigma-Aldrich) for 10 minutes. Images were taken with an inverted microscope (Leica DMi8) using a Leica 10X objective.

For electron microscopy analysis, the small intestines were fixed in 2.5% glutaraldehyde in 0.1 M sodium cacodylate, followed by 1% osmium tetroxide in 0.1 M sodium cacodylate. The samples were embedded in epoxy resin (University of Rochester Electron Microscopy Core) and polymerized at 70 °C. Ultrathin sections were cut at 70 nm and stained with uranyl acetate and lead citrate. Sections were examined at 120 KV with a Hitachi 7650 Analytical TEM with an Erlangshen 11 megapixel digital camera and Gatan software for imaging and morphometric analysis.

For *in situ* hybridization, after deparaffinization and rehydration in hybridization buffer (0.9 M NaCl, 0.1% SDS and 20 mM Tris-HCl, pH 7.4), the small intestines were incubated overnight at 50 °C in the dark with Alexa-532-conjugated Eubacteria EUB338 (5′-GCTGCCTCCCGTAGGAGT-3′) probe for bacterial 16S rRNA genes (Jansen et al., 2000). The probe was diluted to final concentration of 1 ng/μl in hybridization solution. The sections were then washed three times with a hybridization solution for 15 min, counterstained with DAPI and mounted using ProLong Gold Antifade Reagent (Invitrogen). The sections were imaged with an inverted microscope (Leica DMi8) using a Leica 10X objective.

Intestinal crypt isolation and organoid culture—Intestinal organoids were generated from the small intestine as previously described (Sato et al., 2009). Briefly, the proximal small intestine was dissected, rinsed with PBS, minced and incubated in 2.5mM EDTA in PBS for 30 minutes at 4°C with gentle agitation. This mixture was passed through a 70μm cell strainer and pelleted. Isolated crypts were resuspended in Matrigel (Corning) and plated

in 50μl drops on pre-warmed wells in a 24 well plate. After polymerization, 500μL of complete growth medium (Advanced DMEM/F-12 supplemented with EGF (Peprotech), Noggin (Peprotech), N2 (Life Technologies), B27 (Life Technologies), Glutamax (Life Technologies), Penicillin/Streptomycin (Life Technologies), HEPES (Life Technologies), N-Acetylcysteine (Sigma-Aldrich) and R-Spondin) was added and refreshed every 2–3 days.

Quantitative Real-Time PCR—Total RNA was isolated from the small intestines ('segment 8') of naïve or *T. gondii*-infected mice using Trizol (Life Technologies) and subjected to first-strand cDNA synthesis using iScript Reverse Transcription Supermix for RT-qPCR (BioRad). Real-time PCR was performed using Ssofast Eva Green Supermix (BioRad). The relative expression of each sample was determined after normalization to housekeeping gene HPRT using the ddC_t method. The following primers were used for analysis of the gene expression: Cryptdin 2 (Defcr2) 5′-CCAGGCTGATCCTATCCAAA-3′ and 5′-GTCCCATTCATGCGTTCTCT-3′;

Defensin 6 (Defa6) 5'-CCTTCCAGGTCCAGGCTGAT-3'and 5'-TGAGAAGTGGTCATCAGGCAC-3'(Farin et al., 2012); TNF 5'-GCCTCTTCTCATTCCTGCTTGT-3' and 5'- GGCCATTTGGGAACTTCTCAT-3'; Lysozyme 1 (Lyz1) 5'-GCCAAGGTCTACAATCGTTGTGAGTTG-3', 5'-CAGTCAGCCAGCTTGACACCACG-3'; Cre 5'-GATTTCGACCAGGTTCGTTC-3', 5'-GCTAACCAGCGTTTTCGTTC-3'; TNF receptor type I (TNFR1) 5'-GGGCACCTTTACGGCTTCC-3' and 5'-GGTTCTCCTTACAGCCACACA-3'; TNFR2 5'-CAGGTTGTCTTGACACCCTAC-3' and 5'-GCACAGCACATCTGAGCCT-3'; IFN-γ 5'-ACTGGCAAAAGGATGGTGAC-3' and 5'-TGAGCTCATTGAATGCTTGG-3'.

For intestinal microbiota studies, the relative abundancies of Bacteroides, Firmicutes, and Proteobacteria (family *Enterobacteriaceae*) were measured by qPCR with a MyiQ Real-Time PCR Detection System. Bacterial primers used are as follows: Eubacteria 5′-ACTCCTACGGGAGGCAGCAGT-3′ and 5'-ATTACCGCGGCTGCTGGC-3′; γ-Proteobacteria 5′-TAACGCTTGGGAATCTGCCTRTT-3′ and 5′-CATCTRTTAGCGCCAGGCCTTGC- 3′; Bacteroidetes 5′-GGTTCTGAGAGGAGGTCCC-3′ and 5′-GCTGCCTCCCGTAGGAGT-3′; Firmicutes 5′-GGAGYATGTGGTTTAATTCGAAGCA-3′ and 5′-

AGCTGACGACAACCATGCAC-3′ as previously described (Raetz et al., 2013). For *T. gondii* pathogen loads, total genomic DNA from organs was isolated by using the DNeasy Blood and Tissue Kit (Qiagen) according to the manufacturers' instructions. RT-qPCR and downstream analysis were performed as described above. Genomic DNA was compared with a defined copy number standard of the *T. gondii* gene B1. *T. gondii*-specific primers: forward primer 5′- TCCCCTCTGCTGGCGAAAAGT-3′ and reverse primer 5′-AGCGTTCGTGGTCAACTATCGATTG-3′.

***In vivo* intestinal permeability assay—**Intestinal barrier function was assessed by an intestinal permeability assay using a FITC-labeled dextran method, as described previously (Furuta et al., 2001). Briefly, food and water were removed for 4 hours, followed by oral gavage with 60mg/100g body weight of FITC-labeled dextran 4kD (Sigma-Aldrich). Serum

was collected five hours later retro-orbitally and fluorescence intensity was measured (excitation 485nm, emission 528nm). FITC-dextran concentration was calculated using a standard of serially diluted FITC-dextran.

ELISA and serum endotoxin analysis—The IFN-γ concentration in the sera was analyzed by standard sandwich ELISA kit according to manufacturer's instructions (eBioscience). Lipopolysaccharide (LPS) levels in the sera were analyzed using the LAL Chromogenic Endotoxin Quantification kit (Thermo) per manufacturer's instructions.

Measurements of CD4$^+$ T-Cell Responses—To assay the responses of mice infected with *T. gondii*, the mesenteric lymph nodes and spleens were harvested from WT, E-Atg5 KO, and PC-Atg5 KO mice on day 7 post-infection. Single cell suspensions were restimulated with 1 mg/ml αCD3 (BD Biosciences) for 5 hours in the presence of GolgiPlug (Brefeldin A, BD Biosciences). After *in vitro* restimulation, the cells were washed once in PBS + 1% FBS and stained with fluorochrome-conjugated antibodies according to the manufacturer's instructions. For intracellular staining and subsequent washing, cells were permeabilized overnight at 4 °C with the Foxp3/ Transcription Factor Staining Buffer Set according to the manufacturer's instructions (eBioscience). The following antibodies were used for surface or intracellular staining: αCD4 (BD Bioscience; clone GK1.5), αIFN-γ (BD Bioscience; XMG1.2), αTNF (eBioscience; clone MP6-XT22). Cell fluorescence was measured using an LSRII flow cytometer, and data were analyzed using FlowJo software (Tree Star).

Organoid stimulation and imaging—Organoids were stimulated by addition of recombinant murine IFN-γ (100ng/ml; R&D Systems) and/or mTNF-α (5ng/ml; Peprotech) for 24 hours. Organoid death was described when the integrity of the structure was lost and individual cells were seen on the exterior of the organoid. Organoid RNA was isolated using a PureLink RNA Mini Kit (Invitrogen) and subjected to first-strand cDNA synthesis using iScript Reverse Transcription Supermix for RT-qPCR (BioRad). Real-time PCR and downstream analysis was performed as previously described.

For immunofluorescence, organoids were fixed in 4% paraformaldehyde for 2 hours and permeabilized with 0.2% Triton X-100 in PBS for 1 hour at room temperature. Samples were incubated with primary antibody against lysozyme (rabbit polyclonal; Dako) in 0.05% Triton X- 100/PBS for 1 hour. Organoids were then washed and incubated with goat anti-rabbit Alexa Fluor 488 (Molecular Probes) and *Ulex europaeus* agglutinin (UEA) conjugated to TRITC (Sigma-Aldrich) for 1 hour at room temperature. After washing, nuclei were stained with DAPI (Sigma-Aldrich) for 10 minutes. Images of crypt organoids were taken with an inverted microscope (Zeiss AxioVert) using a 40x objective.

Statistical analysis—All data were analyzed with Prism (version 6; Graphpad). These data were considered statistically significant when *P* values were less than 0.05 by two tailed *t* test. Image datasets were processed using Leica Advanced Fluorescence software (Leica) and Image J software (National Institutes of Health).

Supplementary Material

Refer to Web version on PubMed Central for supplementary material.

Acknowledgments

This work was supported by NIAID Grants R56AI085263, R01AI121090, and the Burroughs Wellcome Foundation

References

Adolph TE, Tomczak MF, Niederreiter L, Ko HJ, Bock J, Martinez-Naves E, Glickman JN, Tschurtschenthaler M, Hartwig J, Hosomi S, et al. (2013). Paneth cells as a site of origin for intestinal inflammation. Nature 503, 272–276. [PubMed: 24089213]

Belkaid Y, and Hand TW (2014). Role of the microbiota in immunity and inflammation. Cell 157, 121–141. [PubMed: 24679531]

Benjamin JL, Sumpter R, Jr., Levine B, and Hooper LV (2013). Intestinal epithelial autophagy is essential for host defense against invasive bacteria. Cell host & microbe 13, 723–734. [PubMed: 23768496]

Benson A, Pifer R, Behrendt CL, Hooper LV, and Yarovinsky F (2009). Gut commensal bacteria direct a protective immune response against Toxoplasma gondii. Cell Host Microbe 6, 187–196. [PubMed: 19683684]

Bevins CL, and Salzman NH (2011). Paneth cells, antimicrobial peptides and maintenance of intestinal homeostasis. Nat Rev Microbiol 9, 356–368. [PubMed: 21423246]

Cadwell K, Liu JY, Brown SL, Miyoshi H, Loh J, Lennerz JK, Kishi C, Kc W, Carrero JA, Hunt S, et al. (2008). A key role for autophagy and the autophagy gene Atg16l1 in mouse and human intestinal Paneth cells. Nature 456, 259–263. [PubMed: 18849966]

Cadwell K, Patel KK, Komatsu M, Virgin H.W.t., and Stappenbeck TS (2009a). A common role for Atg16L1, Atg5 and Atg7 in small intestinal Paneth cells and Crohn disease. Autophagy 5, 250–252. [PubMed: 19139628]

Cadwell K, Stappenbeck TS, and Virgin HW (2009c). Role of autophagy and autophagy genes in inflammatory bowel disease. Current topics in microbiology and immunology 335, 141–167. [PubMed: 19802564]

Choi J, Park S, Biering SB, Selleck E, Liu CY, Zhang X, Fujita N, Saitoh T, Akira S, Yoshimori T, et al. (2014). The parasitophorous vacuole membrane of Toxoplasma gondii is targeted for disruption by ubiquitin-like conjugation systems of autophagy. Immunity 40, 924–935. [PubMed: 24931121]

Clevers HC, and Bevins CL (2013). Paneth cells: maestros of the small intestinal crypts. Annual review of physiology 75, 289–311.

Clough B, Wright JD, Pereira PM, Hirst EM, Johnston AC, Henriques R, and Frickel EM (2016). K63-Linked Ubiquitination Targets Toxoplasma gondii for Endo-lysosomal Destruction in IFNgamma-Stimulated Human Cells. PLoS Pathog 12, e1006027. [PubMed: 27875583]

Coers J, and Haldar AK (2015). Ubiquitination of pathogen-containing vacuoles promotes host defense to Chlamydia trachomatis and Toxoplasma gondii. Commun Integr Biol 8, e1115163. [PubMed: 27066178]

Conway KL, Kuballa P, Song JH, Patel KK, Castoreno AB, Yilmaz OH, Jijon HB, Zhang M, Aldrich LN, Villablanca EJ, et al. (2013). Atg16l1 is required for autophagy in intestinal epithelial cells and protection of mice from Salmonella infection. Gastroenterology 145, 1347–1357. [PubMed: 23973919]

Deretic V, and Levine B (2009). Autophagy, immunity, and microbial adaptations. Cell host & microbe 5, 527–549. [PubMed: 19527881]

Deretic V, Saitoh T, and Akira S (2013). Autophagy in infection, inflammation and immunity. Nat Rev Immunol 13, 722–737. [PubMed: 24064518]

Deuring JJ, Fuhler GM, Konstantinov SR, Peppelenbosch MP, Kuipers EJ, de Haar C, and van der Woude CJ (2014). Genomic ATG16L1 risk allele-restricted Paneth cell ER stress in quiescent Crohn's disease. Gut 63, 1081–1091. [PubMed: 23964099]

Dong X, and Levine B (2013). Autophagy and viruses: adversaries or allies? J Innate Immun 5, 480–493. [PubMed: 23391695]

Dudakov JA, Hanash AM, and van den Brink MR (2015). Interleukin-22: immunobiology and pathology. Annu Rev Immunol 33, 747–785. [PubMed: 25706098]

Egan CE, Craven MD, Leng J, Mack M, Simpson KW, and Denkers EY (2009). CCR2-dependent intraepithelial lymphocytes mediate inflammatory gut pathology during Toxoplasma gondii infection. Mucosal Immunol 2, 527–535. [PubMed: 19741601]

Farin HF, Karthaus WR, Kujala P, Rakhshandehroo M, Schwank G, Vries RG, Kalkhoven E, Nieuwenhuis EE, and Clevers H (2014). Paneth cell extrusion and release of antimicrobial products is directly controlled by immune cell-derived IFN-gamma. The Journal of experimental medicine 211, 1393–1405. [PubMed: 24980747]

Farin HF, Van Es JH, and Clevers H (2012). Redundant sources of Wnt regulate intestinal stem cells and promote formation of Paneth cells. Gastroenterology 143, 1518–1529 e1517. [PubMed: 22922422]

Feng CG, Zheng L, Lenardo MJ, and Sher A (2009). Interferon-inducible immunity-related GTPase Irgm1 regulates IFN gamma-dependent host defense, lymphocyte survival and autophagy. Autophagy 5, 232–234. [PubMed: 19066452]

Furuta GT, Turner JR, Taylor CT, Hershberg RM, Comerford K, Narravula S, Podolsky DK, and Colgan SP (2001). Hypoxia-inducible factor 1-dependent induction of intestinal trefoil factor protects barrier function during hypoxia. J Exp Med 193, 1027–1034. [PubMed: 11342587]

Gupta M, Shin DM, Ramakrishna L, Goussetis DJ, Platanias LC, Xiong H, Morse HC, 3rd, and Ozato K (2015). IRF8 directs stress-induced autophagy in macrophages and promotes clearance of Listeria monocytogenes. Nat Commun 6, 6379. [PubMed: 25775030]

Gutierrez MG, Master SS, Singh SB, Taylor GA, Colombo MI, and Deretic V (2004). Autophagy is a defense mechanism inhibiting BCG and Mycobacterium tuberculosis survival in infected macrophages. Cell 119, 753–766. [PubMed: 15607973]

Hara T, Nakamura K, Matsui M, Yamamoto A, Nakahara Y, Suzuki-Migishima R, Yokoyama M, Mishima K, Saito I, Okano H, and Mizushima N (2006). Suppression of basal autophagy in neural cells causes neurodegenerative disease in mice. Nature 441, 885–889. [PubMed: 16625204]

Harris J (2011). Autophagy and cytokines. Cytokine 56, 140–144. [PubMed: 21889357]

Heiseke A, Aguib Y, and Schatzl HM (2010). Autophagy, prion infection and their mutual interactions. Curr Issues Mol Biol 12, 87–97. [PubMed: 19767652]

Hernandez LD, Pypaert M, Flavell RA, and Galan JE (2003). A Salmonella protein causes macrophage cell death by inducing autophagy. J Cell Biol 163, 1123–1131. [PubMed: 14662750]

Ivanov II, McKenzie BS, Zhou L, Tadokoro CE, Lepelley A, Lafaille JJ, Cua DJ, and Littman DR (2006). The orphan nuclear receptor RORgammat directs the differentiation program of proinflammatory IL-17+ T helper cells. Cell 126, 1121–1133. [PubMed: 16990136]

Jansen GJ, Mooibroek M, Idema J, Harmsen HJ, Welling GW, and Degener JE (2000). Rapid identification of bacteria in blood cultures by using fluorescently labeled oligonucleotide probes. J Clin Microbiol 38, 814–817. [PubMed: 10655390]

Jia K, Thomas C, Akbar M, Sun Q, Adams-Huet B, Gilpin C, and Levine B (2009). Autophagy genes protect against Salmonella typhimurium infection and mediate insulin signaling-regulated pathogen resistance. Proceedings of the National Academy of Sciences of the United States of America 106, 14564–14569. [PubMed: 19667176]

Kaiko GE, and Stappenbeck TS (2014). Host-microbe interactions shaping the gastrointestinal environment. Trends Immunol 35, 538–548. [PubMed: 25220948]

Kaser A, and Blumberg RS (2014). ATG16L1 Crohn's disease risk stresses the endoplasmic reticulum of Paneth cells. Gut 63, 1038–1039. [PubMed: 24304670]

Kelsall BL (2008). Innate and adaptive mechanisms to control [corrected] pathological intestinal inflammation. J Pathol 214, 242–259. [PubMed: 18161750]

Kimmey JM, Huynh JP, Weiss LA, Park S, Kambal A, Debnath J, Virgin HW, and Stallings CL (2015). Unique role for ATG5 in neutrophil-mediated immunopathology during M. tuberculosis infection. Nature 528, 565–569. [PubMed: 26649827]

Kirkland D, Benson A, Mirpuri J, Pifer R, Hou B, DeFranco AL, and Yarovinsky F (2012). B cell-intrinsic MyD88 signaling prevents the lethal dissemination of commensal bacteria during colonic damage. Immunity 36, 228–238. [PubMed: 22306056]

Lassen KG, Kuballa P, Conway KL, Patel KK, Becker CE, Peloquin JM, Villablanca EJ, Norman JM, Liu TC, Heath RJ, et al. (2014). Atg16L1 T300A variant decreases selective autophagy resulting in altered cytokine signaling and decreased antibacterial defense. Proc Natl Acad Sci U S A 111, 7741–7746. [PubMed: 24821797]

Lassen KG, McKenzie CI, Mari M, Murano T, Begun J, Baxt LA, Goel G, Villablanca EJ, Kuo SY, Huang H, et al. (2016). Genetic Coding Variant in GPR65 Alters Lysosomal pH and Links Lysosomal Dysfunction with Colitis Risk. Immunity 44, 1392–1405. [PubMed: 27287411]

Lee Y, Sasai M, Ma JS, Sakaguchi N, Ohshima J, Bando H, Saitoh T, Akira S, and Yamamoto M (2015). p62 Plays a Specific Role in Interferon-gamma-Induced Presentation of a Toxoplasma Vacuolar Antigen. Cell Rep 13, 223–233. [PubMed: 26440898]

Levine B, Mizushima N, and Virgin HW (2011). Autophagy in immunity and inflammation. Nature 469, 323–335. [PubMed: 21248839]

Liesenfeld O (2002). Oral infection of C57BL/6 mice with Toxoplasma gondii: a new model of inflammatory bowel disease? J Infect Dis 185 Suppl 1, S96–101. [PubMed: 11865446]

Liesenfeld O, Kang H, Park D, Nguyen TA, Parkhe CV, Watanabe H, Abo T, Sher A, Remington JS, and Suzuki Y (1999). TNF-alpha, nitric oxide and IFN-gamma are all critical for development of necrosis in the small intestine and early mortality in genetically susceptible mice infected perorally with Toxoplasma gondii. Parasite Immunol 21, 365–376. [PubMed: 10417671]

Ling YM, Shaw MH, Ayala C, Coppens I, Taylor GA, Ferguson DJ, and Yap GS (2006). Vacuolar and plasma membrane stripping and autophagic elimination of Toxoplasma gondii in primed effector macrophages. J Exp Med 203, 2063–2071. [PubMed: 16940170]

Liu B, Gulati AS, Cantillana V, Henry SC, Schmidt EA, Daniell X, Grossniklaus E, Schoenborn AA, Sartor RB, and Taylor GA (2013). Irgm1-deficient mice exhibit Paneth cell abnormalities and increased susceptibility to acute intestinal inflammation. Am J Physiol Gastrointest Liver Physiol 305, G573–584. [PubMed: 23989005]

Madison BB, Dunbar L, Qiao XT, Braunstein K, Braunstein E, and Gumucio DL (2002). Cis elements of the villin gene control expression in restricted domains of the vertical (crypt) and horizontal (duodenum, cecum) axes of the intestine. J Biol Chem 277, 33275–33283 [PubMed: 12065599]

Matsuzawa T, Kim BH, Shenoy AR, Kamitani S, Miyake M, and Macmicking JD (2012). IFN-gamma elicits macrophage autophagy via the p38 MAPK signaling pathway. J Immunol 189, 813–818. [PubMed: 22675202]

McSorley SJ, and Bevins CL (2013). Paneth cells: targets of friendly fire. Nat Immunol 14, 114–116. [PubMed: 23334825]

Mizushima N (2002). [Molecular mechanism of autophagy: the role of the Apg12 conjugation system]. Seikagaku. The Journal of Japanese Biochemical Society 74, 523–537. [PubMed: 12187785]

Mizushima N (2007). Autophagy: process and function. Genes & development 21, 2861–2873.

Mizushima N (2009). Methods for monitoring autophagy using GFP-LC3 transgenic mice. Methods in enzymology 452, 13–23. [PubMed: 19200873]

Mizushima N, Yamamoto A, Matsui M, Yoshimori T, and Ohsumi Y (2004). In vivo analysis of autophagy in response to nutrient starvation using transgenic mice expressing a fluorescent autophagosome marker. Mol Biol Cell 15, 1101–1111. [PubMed: 14699058]

Ouellette AJ (2010). Paneth cells and innate mucosal immunity. Curr Opin Gastroenterol 26, 547–553. [PubMed: 20693892]

Patel KK, and Stappenbeck TS (2013). Autophagy and intestinal homeostasis. Annual review of physiology 75, 241–262.

Peterson LW, and Artis D (2014). Intestinal epithelial cells: regulators of barrier function and immune homeostasis. Nature reviews. Immunology 14, 141–153.

Py BF, Lipinski MM, and Yuan J (2007). Autophagy limits Listeria monocytogenes intracellular growth in the early phase of primary infection. Autophagy 3, 117–125. [PubMed: 17204850]

Raetz M, Hwang SH, Wilhelm CL, Kirkland D, Benson A, Sturge CR, Mirpuri J, Vaishnava S, Hou B, Defranco AL, et al. (2013). Parasite-induced TH1 cells and intestinal dysbiosis cooperate in IFN-

gamma-dependent elimination of Paneth cells. Nature immunology 14, 136–142. [PubMed: 23263554]

Rioux JD, Xavier RJ, Taylor KD, Silverberg MS, Goyette P, Huett A, Green T, Kuballa P, Barmada MM, Datta LW, et al. (2007). Genome-wide association study identifies new susceptibility loci for Crohn disease and implicates autophagy in disease pathogenesis. Nature genetics 39, 596–604. [PubMed: 17435756]

Salas A, and Panes J (2009). Defects in autophagy induce alterations in the secretory pathway and proinflammatory signaling of paneth cells. Gastroenterology 137, 1527–1529. [PubMed: 19717131]

Salzman NH, Hung K, Haribhai D, Chu H, Karlsson-Sjoberg J, Amir E, Teggatz P, Barman M, Hayward M, Eastwood D, et al. (2010). Enteric defensins are essential regulators of intestinal microbial ecology. Nature immunology 11, 76–83. [PubMed: 19855381]

Salzman NH, Underwood MA, and Bevins CL (2007). Paneth cells, defensins, and the commensal microbiota: a hypothesis on intimate interplay at the intestinal mucosa. Seminars in immunology 19, 70–83. [PubMed: 17485224]

Sato T, Vries RG, Snippert HJ, van de Wetering M, Barker N, Stange DE, van Es JH, Abo A, Kujala P, Peters PJ, and Clevers H (2009). Single Lgr5 stem cells build crypt-villus structures in vitro without a mesenchymal niche. Nature 459, 262–265. [PubMed: 19329995]

Selleck EM, Orchard RC, Lassen KG, Beatty WL, Xavier RJ, Levine B, Virgin HW, and Sibley LD (2015). A Noncanonical Autophagy Pathway Restricts Toxoplasma gondii Growth in a Strain-Specific Manner in IFN-gamma-Activated Human Cells. MBio 6, e01157–01115. [PubMed: 26350966]

Stappenbeck TS (2010). The role of autophagy in Paneth cell differentiation and secretion. Mucosal immunology 3, 8–10. [PubMed: 19890269]

Stappenbeck TS, and McGovern DP (2016). Paneth Cell Alterations in the Development and Phenotype of Crohn's Disease. Gastroenterology.

Strober W, Fuss I, and Mannon P (2007). The fundamental basis of inflammatory bowel disease. J Clin Invest 117, 514–521. [PubMed: 17332878]

Van Grol J, Muniz-Feliciano L, Portillo JA, Bonilha VL, and Subauste CS (2013). CD40 induces anti-Toxoplasma gondii activity in nonhematopoietic cells dependent on autophagy proteins. Infection and immunity 81, 2002–2011. [PubMed: 23509150]

Weaver CT, Elson CO, Fouser LA, and Kolls JK (2013). The Th17 pathway and inflammatory diseases of the intestines, lungs, and skin. Annu Rev Pathol 8, 477–512. [PubMed: 23157335]

Zhang Q, Pan Y, Yan R, Zeng B, Wang H, Zhang X, Li W, Wei H, and Liu Z (2015). Commensal bacteria direct selective cargo sorting to promote symbiosis. Nature immunology 16, 918–926. [PubMed: 26237551]

Zhao Z, Fux B, Goodwin M, Dunay IR, Strong D, Miller BC, Cadwell K, Delgado MA, Ponpuak M, Green KG, et al. (2008). Autophagosome-independent essential function for the autophagy protein Atg5 in cellular immunity to intracellular pathogens. Cell Host Microbe 4, 458–469. [PubMed: 18996346]

Highlights

- Basal Paneth cell autophagy is driven by the microbiota and IFN-γ
- Paneth cell autophagy protects against acute infection
- Loss of Paneth cell autophagy results in impaired intestinal permeability
- Loss of Paneth cell autophagy leads to TNF- and IFN-γ mediated intestinal pathology

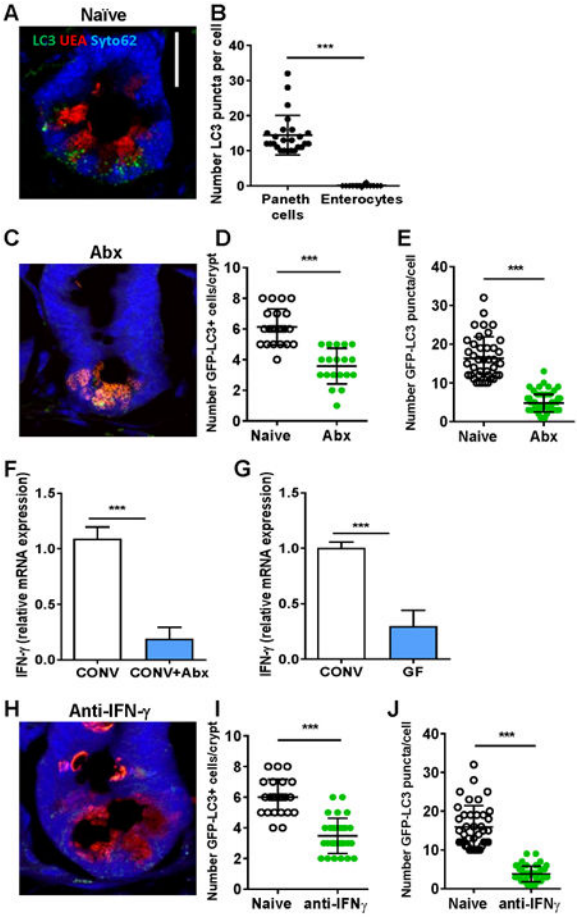

Figure 1: Paneth cell autophagy is microbiota- and IFN-γ-dependent.

(A) Immunofluorescence of intestinal crypts of naïve GFP-LC3 mice for Paneth cells (UEA, red), LC3 (green), and nucleic acid (Syto62, blue). Bar = 20um. Results are representative of three independent experiments. (B) Quantification of GFP-LC3+ cells in the Paneth cells and enterocytes in the intestinal epithelium from naïve (n=3) mice. Results are representative of three independent experiments. ***P<0.0001. (C) Mice were treated with antibiotic water (ampicillin, streptomycin, neomycin, metronidazole, vancomycin) for 10 days and analyzed by immunofluorescence for Paneth cells (UEA, red), LC3 (green), and nucleic acid (Syto62, blue). Quantification of number of GFP-LC3+ cells per crypt (D) and number of GFP-LC3+ puncta per cell (E) in naïve (white) and antibiotic treated (green) mice. The results are representative of three independent experiments involving at least three mice per group. ***P<0.0001. Data shown are mean ± s.d. (F) qRT-PCR analysis of relative IFN-γ expression, measured in the small intestines of control (CONV), antibiotic-treated mice (CONV+Abx), and (G) microbiologically sterile germ-free (GF) mice (n=6) (H) Mice were treated with anti-IFN-γ blocking antibody and analyzed by immunofluorescence for Paneth cells (UEA, red), LC3 (green), and nucleic acid (Syto62, blue). (I) Quantification of number of GFP-LC3+ cells per crypt and (J) number of GFP-LC3+ puncta per cell in control (white) and treated (green) mice. The results are representative of three independent experiments involving at least three mice per group. ***P<0.0001. Data shown are mean ± s.d.

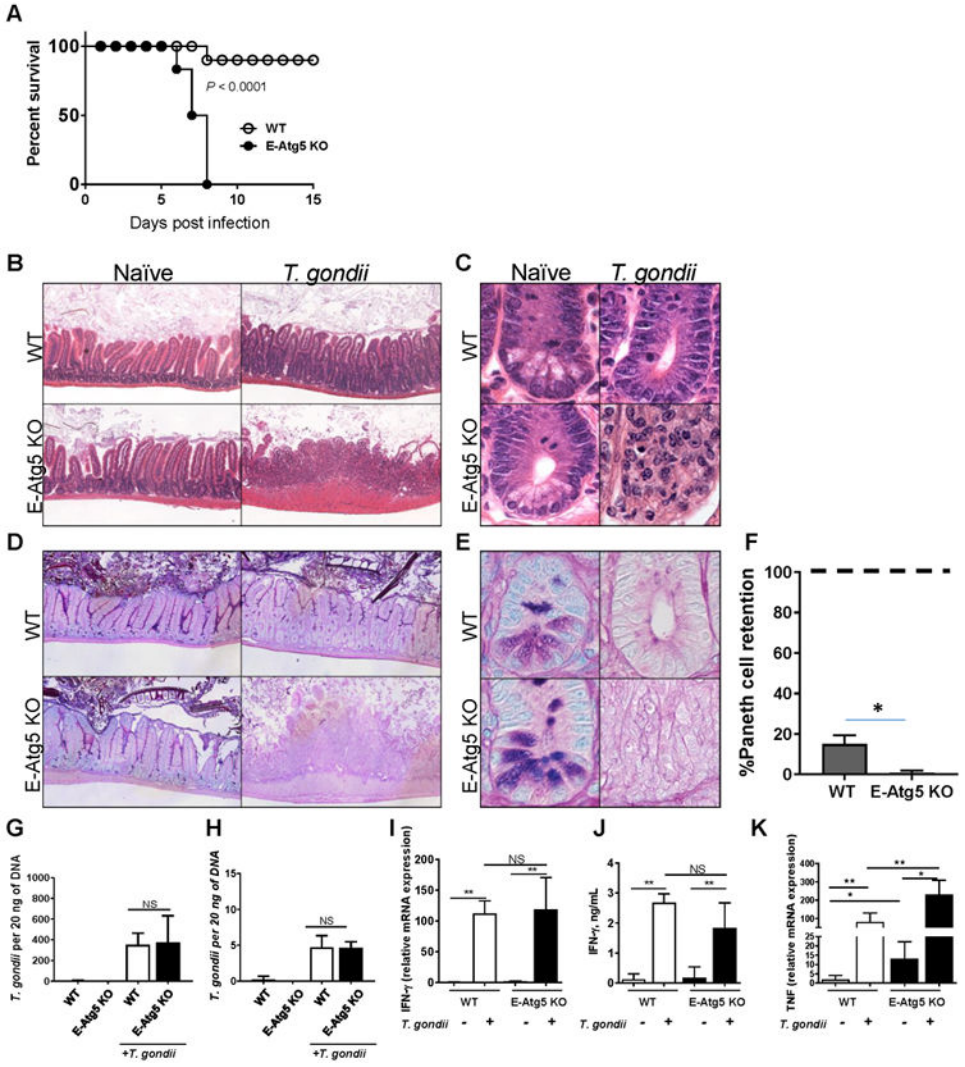

Figure 2: Loss of intestinal epithelial autophagy increases immunopathology in response to *T. gondii*.

(A) Survival of WT (open circles) and E-Atg5 KO (black circles) mice during oral infection with 20 cysts ME49 *T. gondii* from a combination of three experiments, each involving at least three mice per group. $P<0.0001$. Histological analysis of small intestines of naïve and infected WT and E-Atg5 KO mice with 20 cysts of ME49 *T. gondii* on day 7 by (B,C) H&E and (D,E) Alcian Blue/PAS staining at 10x (B,D) and 40x (C,E). Image fields are representative of pathology in multiple tissue sections, and chosen sections were selected by blinded observation. (F) Quantification of number of Paneth cells in *T. gondii*-infected WT and E-Atg5 KO mice on day 7 post infection. Quantification of number of Paneth cells in naïve mice (100%) is marked by the dotted line. Paneth cells were identified based on their morphology of large granule-containing cells and a basolateral nucleus at the base of the intestinal crypt. (G) Analysis of *T. gondii* parasite loads by qRT-PCR in spleen and (H) liver. (I) qRT-PCR for IFN-γ transcript in the small intestine and (J) ELISA for IFN-γ in sera of naïve and *T. gondii*-infected mice. (K) qRT-PCR analysis of relative small intestinal TNF.

Results are representative of four independent experiments involving at least four mice per group. *P<0.05, **P<0.005. NS = not significant, error bars = mean ± s.d.

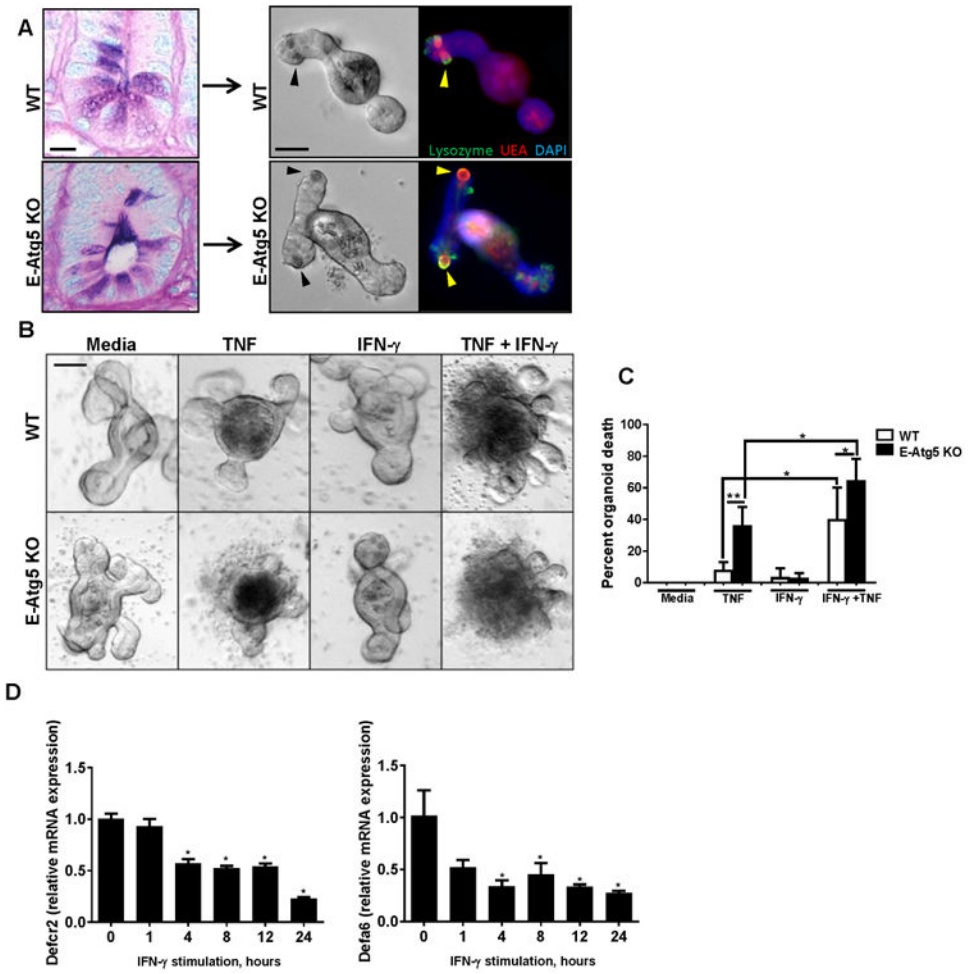

Figure 3: Intestinal organoids lacking Atg5 are more sensitive to cytokine-mediated death.

(A) Intestinal organoids were generated from small intestinal stem cells isolated from crypts of WT and E-Atg5 KO mice (left, scale bar 10 μm). Paneth cells were visualized by light microscopy (center panel, black arrowheads) and immunofluorescence (yellow arrowheads indicating colocalization of Paneth cell markers UEA (red) and lysozyme (green), scale bar 50μm). (B) Organoids were stimulated with TNF (5ng/ml), IFN-γ (100ng/ml), or both cytokines for 12 hours and imaged by light microscopy. Scale bar 50 μm (C) Quantification of death in WT and E-Atg5 KO organoids, characterized by loss of epithelial integrity by light microscopy. (D) qRT-PCR analysis of organoids stimulated with IFN-γ (100ng/ml) for relative Defcr2 and Defa6 expression. Results are representative of four independent experiments involving at least four mice per group. **P*<0.05, **P*<0.005. Data shown are mean ± s.d.

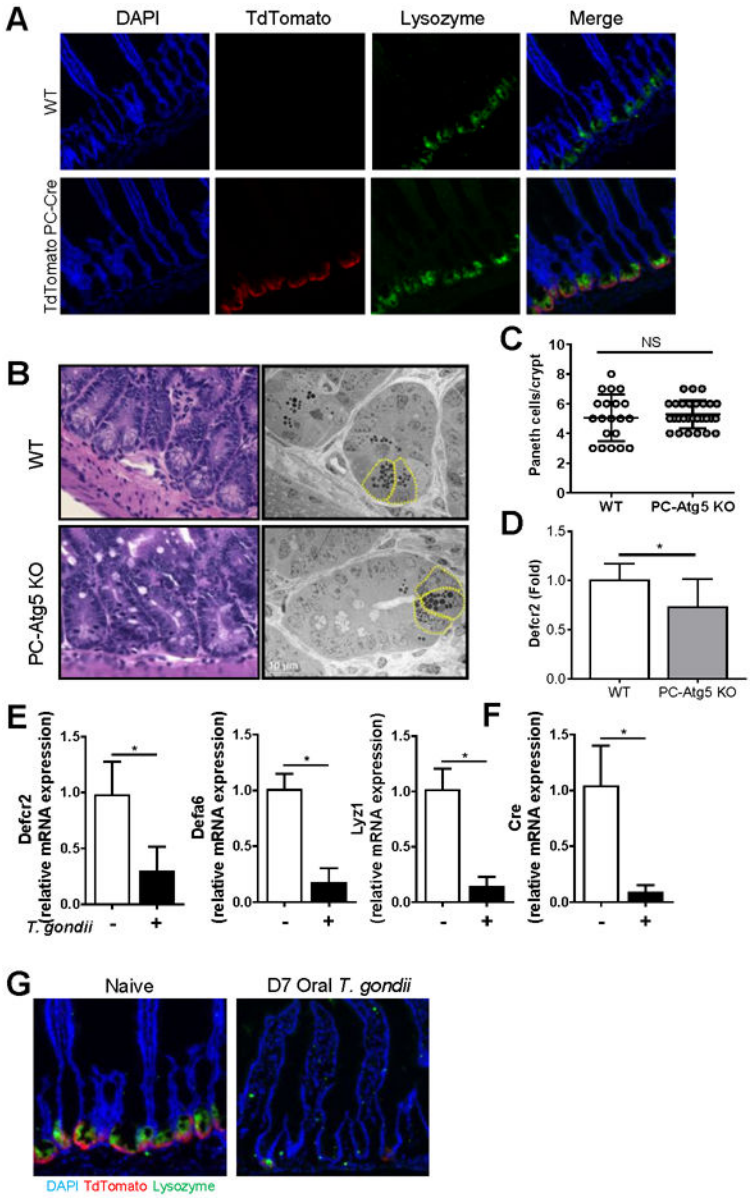

Figure 4: Generation of Paneth cell-specific autophagy-deficient mice.

(A) Representative images of *TdTomato-Rosa26/Defa4-cre* reporter mice and WT (controls). Co-localization of *Defa4* Cre-driven TdTomato expression (red) with lysozyme-expressing Paneth cells (green) and DAPI (blue). (B) Representative hematoxylin and eosin (left) and TEM images (right) of WT and PC-Atg5 KO small intestines. Granule-filled Paneth cells outlined in yellow. (C) Quantification of Paneth cells per crypt in naïve WT and PC-Atg5 KO mice and (D) qRT-PCR analysis of relative small intestinal Defcr2 expression. (E) qRT-PCR analysis for relative Defcr2, Defa6 and Lyz1 expression and (F) Cre transcripts in naïve and *T. gondii*-infected *TdTomato-Rosa26/Defa4-cre* mice. (G) Representative images of naïve and *T. gondii*-infected *TdTomato-Rosa26/Defa4-cre* mice, counter-stained with lysozyme (green) and DAPI (blue). Results are representative of four independent

experiments involving at least four mice per group. *P<0.05, NS = not significant, data shown are mean ± s.d.

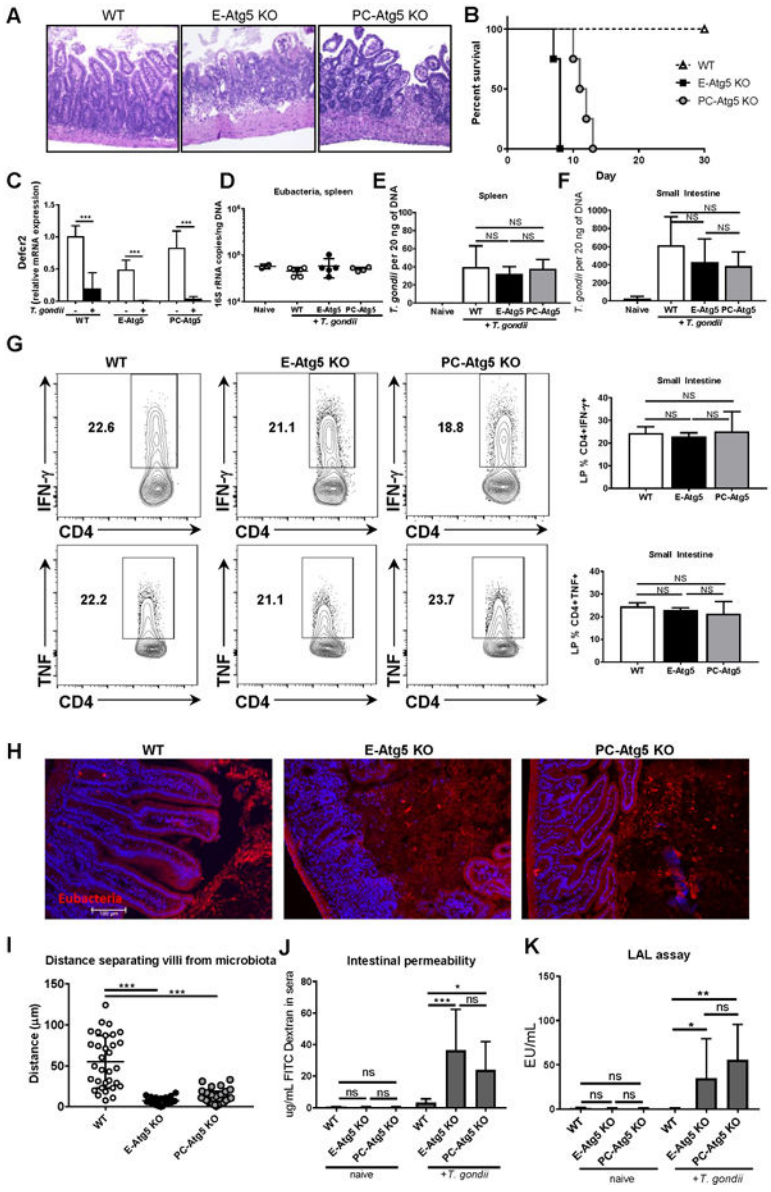

Figure 5: Immunopathology of Atg5 deficiency originates from Paneth cells.

(A) Representative 10x H&E images of WT, E-Atg5 KO, and PC-Atg5 KO mice on day 7 post infection. (B) Survival of WT, E-Atg5 KO and PC-Atg5 KO mice during oral infection with 20 cysts ME49 *T. gondii*, representative of three experiments each involving at least four mice per group. (C) qRT-PCR analysis of relative small intestinal Defcr2 expression in naïve or *T. gondii*-infected WT, E-Atg5 KO, and PC-Atg5 KO mice. (D) qRT-PCR analysis of Eubacteria loads in the spleen. (E) Analysis of *T. gondii* parasite loads by qRT-PCR in spleen and (F) and small intestine. (G) Flow cytometric analysis and quantification of CD4+ IFN-γ+ and CD4+ TNF+ cells in the small intestinal lamina propria of *T. gondii*-infected WT, E-Atg5 KO, and PC-Atg5 KO mice on day 7 post infection. (H) The distribution of microbiota in the lumens of the small intestines was analyzed by in situ hybridization with Eubacteria-specific (red) probes in mice on day 7 post infection and counterstained with DAPI. Scale bar 100μm. (I) Quantification of distance separating villi from microbiota in *T.*

gondii-infected mice (μm). (J) Detection of FITC fluorescence in sera, four hours after oral gavage with FITC-dextran (4kD) in naïve and *T. gondii*-infected (day 7 post infection) WT, E-Atg5 KO and PC-Atg5 KO mice. (K) Quantification of sera endotoxin levels by LAL assay in naïve and *T. gondii*-infected (day 7 post infection) WT, E-Atg5 KO and PC-Atg5 KO mice. Results are representative of four independent experiments involving at least four mice per group. *$P<0.05$, **$P<0.005$, ***$P<0.0005$ (unpaired two-tailed Student's t test). NS = not significant, data shown are mean ± s.d.

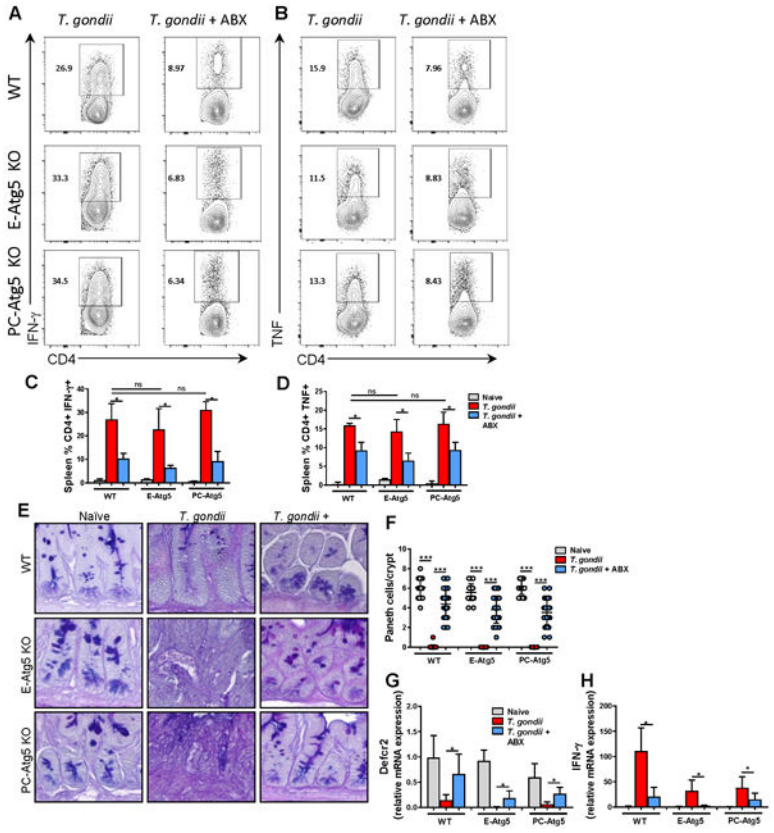

Figure 6: Intestinal inflammation and immunopathology is microbiota-dependent.

(A,B) Flow cytometric analysis and (C,D) quantification of splenic CD4+ IFN-γ+ (A,C) and CD4+ TNF+ (B,D) in *T. gondii*-infected control or antibiotic-treated WT, E-Atg5 KO, and PC-Atg5 KO mice on day 7 post infection. (E) Histologic visualization and (F) quantification of Paneth cells by Alcian Blue/PAS staining of small intestinal crypts in WT, E-Atg5 KO and PC-Atg5 KO mice infected with *T. gondii* and additionally treated with antibiotic drinking water (ampicillin, streptomycin, neomycin, metronidazole, vancomycin) for 10 days. (G) qRT-PCR analysis of relative small intestinal Defcr2 and (H) IFN-γ expression in control and antibiotic-treated WT, E-Atg5 KO and PC-Atg5 KO mice. Results are representative of five independent experiments involving at least four mice per group. **P*<0.05, ****p*<0.0005. NS = not significant, data shown are mean ± s.d.

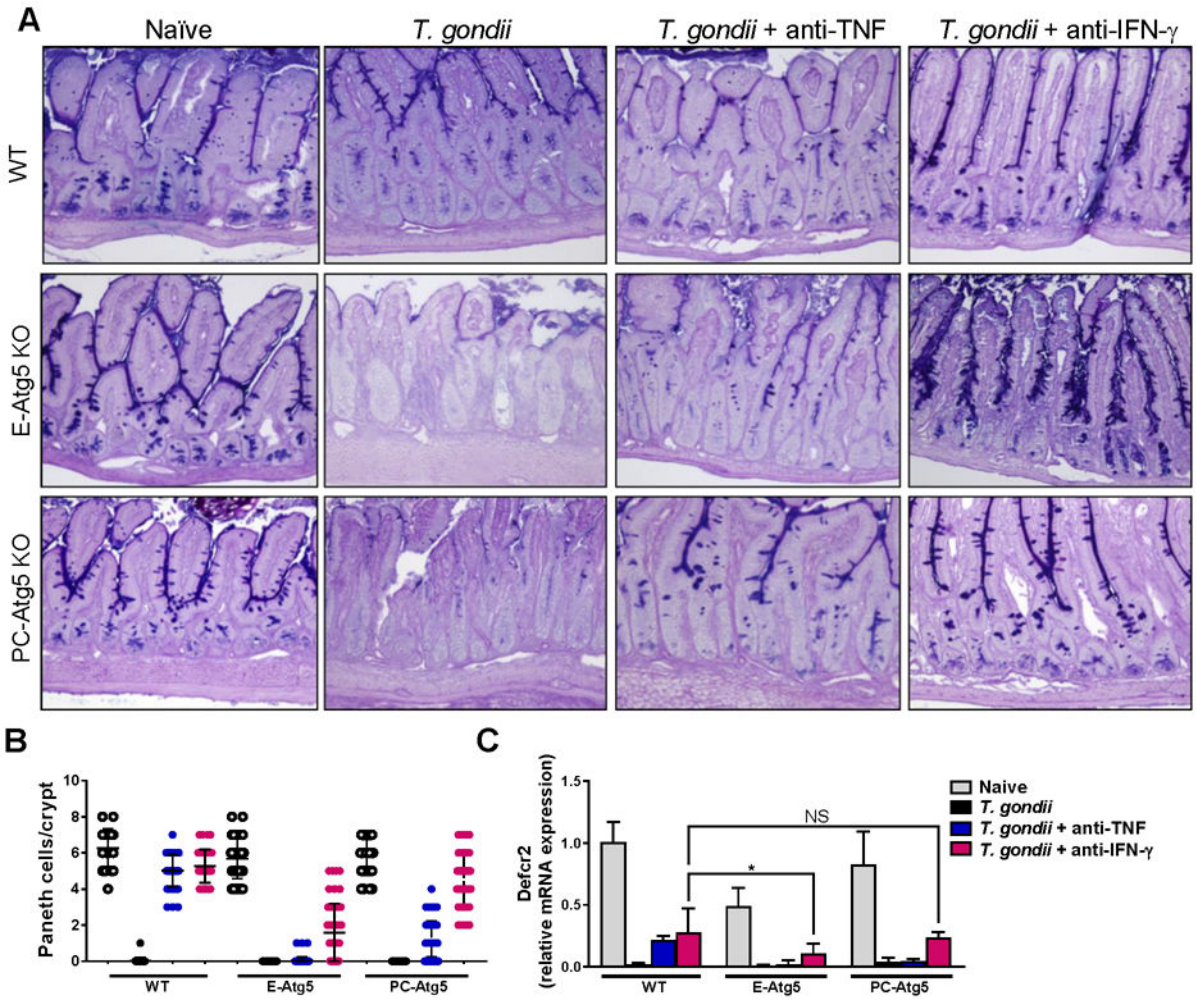

Figure 7: Paneth cell loss and intestinal immunopathology is TNF and IFN-γ-dependent.

(A) Histologic visualization of Paneth cells in naïve or *T. gondii* infected WT, E-Atg5 KO, and PC-Atg5 KO mice by Alcian Blue/PAS staining. WT, E-Atg5 KO, and PC-Atg5 KO mice were treated with anti-IFN-γ or anti-TNF and then infected orally with 20 cysts per mouse of the ME49 strain of *T. gondii*. Histological analyses of Paneth cells in small intestines were performed on day 7 after infection as described above. (B) Paneth cell quantification and (C) qRT-PCR analysis of relative small intestinal Defcr2 expression in naïve or *T. gondii*-infected WT, E-Atg5 KO, and PC-Atg5 KO mice. Results are representative of four independent experiments involving at least four mice per group. **P*<0.05, ****P*<0.0005. NS = not significant, data shown are mean ± s.d.